12WCEE 2000

ANALYTICAL METHOD FOR PREDICTING THE RESPONSE OF TIED CONCRETE COLUMNS TO SEISMIC LOADING

Beni ASSA[1], Fumio WATANABE[2] And Minehiro NISHIYAMA[3]

SUMMARY

This paper presents an analytical method for the prediction of load-displacement curve of reinforced concrete beam-columns subjected to simulated seismic loading. The method to predict the flexural deformation is based on finite element approach which allows for the spreading of inelasticity along the member. The effect of lateral confinement by transverse reinforcement was included in the uniaxial stress-strain relations of confined core concrete. A new approach for predicting the stress-strain curve of confined concrete was also included in this paper.

An analytical method to determine the deformation due to slippage of reinforcing steels from the beam to column joint was developed. The method was based on finite element approach utilizing the bond-slip behaviour of steel bar embedded in concrete. The deformation component associated with shear was calculated using the method available in the literature.

The accuracy of predictions of the method have been verified by comparing the hysteretic load displacement curves obtained from the computer program with the experimental results published in the literatures. This comparative study indicated that the analytical method presented in this paper is capable of predicting the response of reinforced concrete beam-columns to seismic loading with sufficient accuracy.

INTRODUCTION

The response of Reinforced Concrete(RC) beam-column to seismic loading is commonly represented by its load-displacement curve under combined axial and lateral cyclic loading. This curve is an important information from which the ductility and energy dissipation behaviours of RC beam-columns can be determined.

This paper describes an analytical method for predicting the load-displacement curve of RC beam-columns subjected to axial load and uniaxial bending (both monotonic and cyclic loading). Three deformation components namely flexural, bar slip and shear deformation were considered in the analysis. The uniaxial stress-strain relations of the constituent materials namely steel and concrete are required for the purpose.

Stress-strain behaviour of confined concrete within the core, significantly affects the load-displacement curve of RC beam-column, particularly at large deformation state. An analytical method for predicting the stress-strain curve of confined core concrete is also presented in this paper. A confinement model was developed based on the concrete-confining steel interaction and the compatibility in the lateral expansion.

[1] *Associate Professor, Dept of Civil Eng, Sam Ratulangi University, Indonesia. e-mail bennyrc@mdo.mega.net.id*
[2] *Professor, Dept of Architecture and Systems, Kyoto University, Japan. e-mail nabe@archi.kyoto-u.ac.jp*
[3] *Associate Professor, Dept of Architecture and Systems, Kyoto University, Japan. e-mail mn@archi.kyoto-u.ac.jp*

2. FLEXURAL ANALYSIS OF RC BEAM-COLUMNS

A beam-column with central stub shown in Fig.1. is used as an example problem for the purpose of describing the method. This form of specimen is generally used by researchers in their experimental investigations to study the behaviour of RC beam-columns subjected to monotonically and cyclically varying axial and lateral loading.

The RC beam-column is divided into a number of finite line elements along its longitudinal axis including two plastic hinge elements on both sides of the central stub. A RC beam-column finite element with a number of integration sections is schematically shown in Fig.2. Each section is discretized into layers defined with respect to the member axis. Each layer that is either the cover concrete, core concrete or reinforcing steel follows the uniaxial stress-strain relations of material.

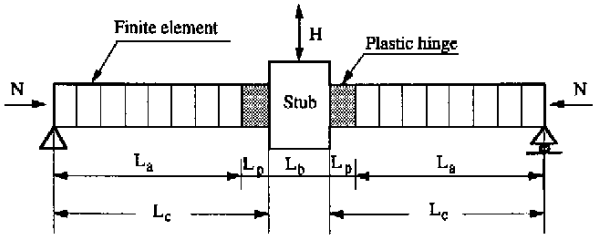

Figure 1: Modelling of RC beam-column

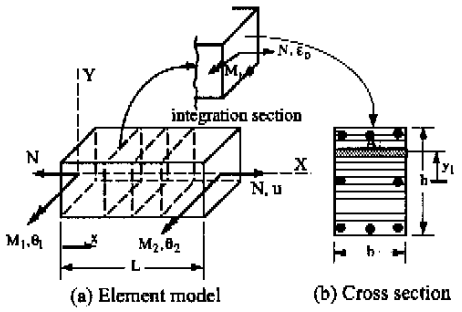

Figure 2: RC beam-column element

Two independent shape functions are used for approximating the force and deformation fields along the element. The section forces $\boldsymbol{R_s}\ (M, N)$ are related to the forces at the ends of the element $\boldsymbol{R_e}\ (M_1, M_2, N)$ using a matrix $\boldsymbol{b}$ and the section deformations increment $\boldsymbol{\Delta D_S}\ (\Delta\phi, \Delta\varepsilon_o)$ are related to the element end deformations increment $\boldsymbol{\Delta D_e}\ (\Delta\theta_1, \Delta\theta_2, \Delta u)$ using a matrix $\boldsymbol{a}$. The force interpolation function $\boldsymbol{b}$ is given by Eq.(1) and a deformation interpolation function $\boldsymbol{a}$ which is flexibility dependent is given by Eq.(2). By such a formulation the stiffness of RC beam-column element can be derived as given by Eqs.(3) and (4).

$$\boldsymbol{b}(x) = \begin{bmatrix} -1+\frac{x}{L} & \frac{x}{L} & 0 \\ 0 & 0 & 1 \end{bmatrix} \tag{1}$$

$$\boldsymbol{a}(x) = \boldsymbol{f}(x)\,\boldsymbol{b}(x)\,[\boldsymbol{F}]^{-1} \tag{2}$$

$$\boldsymbol{F} = \int_0^L \boldsymbol{b}^T(x)\,\boldsymbol{f}(x)\,\boldsymbol{b}(x)\,dx \tag{3}$$

$$\boldsymbol{S_e} = [\boldsymbol{F}]^{-1} \tag{4}$$

in which $\boldsymbol{f}$ = section flexibility matrix; $\boldsymbol{F}$ = element flexibility matrix; $\boldsymbol{S_e}$ = element stiffness matrix. The section flexibility matrix $\boldsymbol{f}$ is determined by simply inverting the section stiffness matrix $\boldsymbol{S_s}$ given in Eq. (5).

$$\boldsymbol{S_s} = \begin{bmatrix} \sum_{i=1}^{n} E_{m,i}\,A_i\,y_i^2 + \sum_{i=1}^{n} E_{m,i}\,I_i & \sum_{i=1}^{n} E_{m,i}\,A_i\,y_i \\ \sum_{i=1}^{n} E_{m,i}\,A_i\,y_i & \sum_{i=1}^{n} E_{m,i}\,A_i \end{bmatrix} \tag{5}$$

in which n=total number of layers; A_i = area of i-th layer; I_i = moment of inertia of i-th layer with reference to its own centroid; y_i = distance from the centroid of the section to the centroid of i-th layer; $E_{m,i}$ = tangent stiffness of i-th layer. The tangent stiffness of concrete (both cover and core) and steel are evaluated from the uniaxial stress-strain relations.

The plastic hinge element is derived by keeping the section deformations (ϕ and ε_o) and forces (M and N)

constant along the full length (L_p) of the element. The interpolation matrix $\boldsymbol{b}$ is equal to 2 x 2 unit matrix. By substituting unit matrix for the matrix $\boldsymbol{b}$ and using L_p for L in Eq.(3) yields

$$\boldsymbol{F} = L_p \, \boldsymbol{f}_s \tag{6}$$

in which $\boldsymbol{f}_s$ is the flexibility matrix of the critical section.

The stiffness of the entire structure is determined by direct assembling of the stiffness matrices of the general beam-column elements and the two plastic hinge elements. This assembly process establishes the equilibrium equations for the entire structure. The beam-column is then analysed for the prescribed axial force (N) and curvature (ϕ) of the critical sections. Incremental iterative technique is used for the solution of the equilibrium equations.

2.1 Stress-Strain Relations of Core Concrete Under Monotonic Compression

The uniaxial stress-strain curve of confined concrete is determined by enforcing compatibility in the lateral expansion between concrete and transverse steel system. The response of transverse steel system to lateral expansion of concrete is represented by the lateral stress-lateral area strain ($f_r - \varepsilon_a$) curve. The lateral area strain is defined as the change in cross sectional area per unit area of original cross section. Deformational behaviour of concrete under axial and lateral compression is represented by a set of constitutive relations.

2.1.1 Constitutive Relations For Concrete

A significant number of concrete cylinders reinforced with spiral or circular hoops were tested at the Kyoto University, Japan, under both monotonic and cyclic compression to failure. On the basis of this experimental results, a set of constitutive relations for confined concrete was derived as given in Eqs.(7) to (10)

$$\frac{f_{cc}}{f_c'} = 1 + 3.36 \frac{f_{rp}}{f_c'} \tag{7}$$

$$\frac{\varepsilon_{cc}}{\varepsilon_{uc}} = 1.0 + 21.5 \frac{f_{rp}}{f_c'} \tag{8}$$

$$\frac{\varepsilon_{80}}{\varepsilon_{uc}} = 2.80 + 40.00 \frac{f_{rp}}{f_c'} \tag{9}$$

$$\varepsilon_{ap} = 0.0042 + 0.0320 \frac{f_{rp}}{f_c'} \tag{10}$$

in which f_{cc} = maximum axial stress; ε_{cc} = axial strain at maximum axial stress; ε_{ap} = lateral area strain at peak; ε_{80} = axial strain at 20% stress drop on the descending branch; f_{rp} = the attainable lateral stress provided at peak axial load; f_c' = the concrete strength; ε_{uc} = strain at peak of plain concrete cylinder.

2.1.2 Lateral Stress-Lateral Area Strain Curve of Transverse Steel

A reinforced concrete cross section with peripheral hoop is shown in Fig.3.a. The steel bars of the peripheral hoop are divided into a number of column finite elements, whilst the cross-tie (if any) is idealized as an axial element. The concrete is discretized into a number of segments bounded by the peripheral steel bar element and the lines joining the centre point and the middle of two nodes. The concrete segment is represented by an axial compressive element having axial stiffness k_c and zero tensile strength as shown in Fig.3.b.

Stiffness of Concrete Element

A concrete segment and its idealized axial element are shown in Fig.3.c. Point O is assumed to be a pin joint. The stiffness k_c of concrete element is defined as the confining force F_r required to produce a unit compressive deformation ($\Delta r_o = 1$ unit) in the concrete element. It is assumed that the concrete segment is subjected to uniform lateral stress. Therefore, the axial compressive stiffness of the element is given by Eq.(11).

$$k_c = \frac{F_r}{\Delta r_o} = \frac{L_e\, s\, E_{cr}}{r_o} \tag{11}$$

in which s = spacing of the lateral ties; L_e = the width of concrete segment measured perpendicular to the element axis; r_o is the length of concrete element; E_{cr} is the stiffness of concrete in the lateral direction as given in Eq.(12).

$$E_{cr} = \frac{100}{e^{3s/b_c}} \left(f_c'\right)^{1.2} \tag{12}$$

in which e=2.718 and b_c = least lateral dimension of confined concrete core.

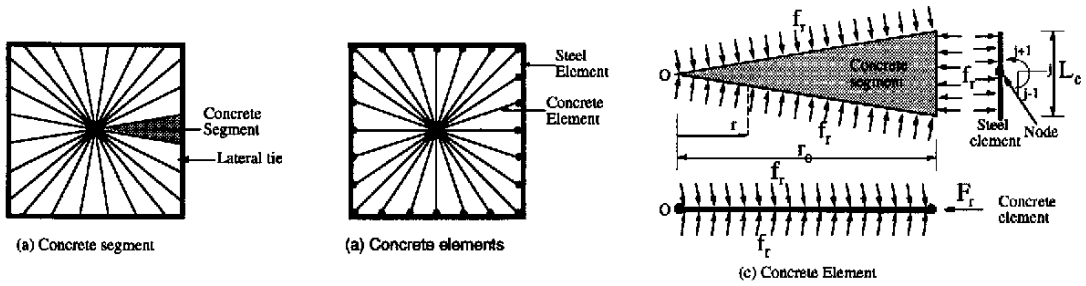

Figure 3: Modelling of Transverse Steel - Concrete Interaction

Stiffness of Steel Element

Two types of element are used to simulate the response of transverse steel system. A column element is used for the peripheral steel bars, whilst an axial element is used for the cross-ties. The column element is similar to the RC beam-column element shown in Fig.2 but having circular cross section. Each section is discretized into layers and each layer follows the uniaxial stress strain relations of reinforcing steel. The stiffness of the peripheral steel element was determined similarly to the RC beam-column element as given in Eqs.(1) to (5), whilst the stiffness of the axial element is given in Eq.(13)

$$S_e = \frac{A_s\, E_s}{L} \tag{13}$$

in which A_s is the cross sectional area of cross-tie and E_s is the tangent stiffness.

The stiffness of the entire transverse steel system is determined by direct assembling of the stiffness matrices of the peripheral steel elements and the axial elements (if any).

Equilibrium Equations

The mechanism of confinement can be simply explained as follows. Let assume first that there is no lateral steel. Under axial compression, the plain concrete expands laterally and reaches its lateral expansion capacity when the axial load approaches the maximum axial load. The presence of lateral steel reduces this lateral expansion by lateral compression, hence delays the axial load reaching its maximum value. This mechanism is illustrated in Fig.4. and formulated in Eqs.(14) and (15)

$$\Delta r_o + \Delta d_r = \Delta \varepsilon_{ro}\, r_o \tag{14}$$

$$\Delta F_r = k_c \left(\Delta \varepsilon_{ro}\, r_o - \Delta d_r\right) \tag{15}$$

in which ε_{ro} is the free lateral tensile strain of plain concrete section (without transverse reinforcement); d_r is the nodal displacement measured in the direction of concrete element; symbol Δ indicates that the equations are in incremental form.

Each node has three degrees of freedom labelled as (j+1), (j) and (j-1) in Fig.4. The lateral deformation and nodal force as given in Eqs.(14) and (15) are decomposed into two components in the direction of (j) and (j-1) coordinates. As the concrete segment is represented by the axial element, there is no interaction between concrete and steel in the rotational coordinate (j+1), hence the corresponding nodal force is zero. By applying Eq.(15) at all nodes produces a set of equilibrium equations in the form of linearized structure's force-deformation increment relations. The solution of those equations is then carried out incrementally and iteratively for a prescribed value of ε_{ro} to produce the $(f_r - \varepsilon_a)$ curve.

2.1.3 Lateral Stress at Peak Axial Load

The lateral expansion of concrete at maximum axial load is represented by a straight line given by Eq.(10). This line is the locus of points corresponding to a pair of lateral stress and lateral area strain values that define the maximum axial stress of confined concrete, hence named the 'Peak Load Condition (PLC) Line'.

The($f_r - \varepsilon_a$) curve represents the potential of the transverse steel of providing the confining pressure to the concrete. By enforcing compatibility in the lateral expansion between concrete and transverse steel at peak axial load, the attainable lateral stress and lateral area strain can be determined from the intersection between the PLC Line and the equivalent lateral stress-area strain ($f_r - \varepsilon_a$) curve. This principle is illustrated in Fig.5. Having the lateral stress at peak axial load (f_{rp}), f_{cc}, ε_{cc} and ε_{80} are calculated from Eqs.(7), (8) and (9) and the stress-strain curve of confined concrete is generated.

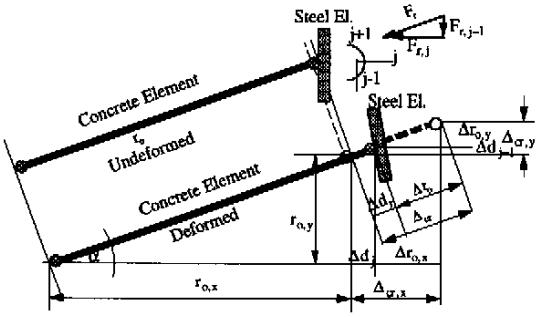

Figure 4: Compatibility at nodes

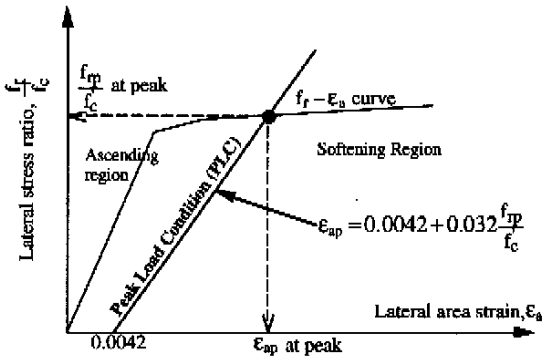

Figure 5: Determination of Lateral Stress at Peak

2.1.4 Uniaxial Stress-Strain Equation For Confined Core Concrete

The equation (16) is used to represent the stress-strain curve of confined concrete.

$$f_c = f_{cc}\frac{\alpha x + (\beta - 1)x^2}{1 + (\alpha - 2)x + \beta x^2} \tag{16}$$

in which :

$$x = \frac{\varepsilon_c}{\varepsilon_{cc}} \tag{17}$$

$$\alpha = \frac{E_c\,\varepsilon_{cc}}{f_{cc}} \tag{18}$$

$$\beta = \frac{x_{80}^2 - (0.2\alpha + 1.6)x_{80} + 0.80}{0.2\,x_{80}^2} \tag{19}$$

$$x_{80} = \frac{\varepsilon_{80}}{\varepsilon_{cc}} \tag{20}$$

$$E_c = 4700\sqrt{f_c'}\ \text{MPa} \tag{21}$$

2.2 Stress-Strain Relations of Cover Concrete Under Monotonic Compression

Stress-strain curves for unconfined cover concrete proposed by Muguruma et al.[1979 1983] are adopted in this study. The ascending branch is given by a parabola with vertex at the maximum stress point equal to the compressive strength of concrete. The softening branch is represented by a straight line.

2.3 Stress-Strain Relations of Concrete Under Cyclic Compression

Based on the experimental results mentioned in the previous section, the hysteretic models schematically shown in Fig.6. were derived to simulate the stress-strain relations of concrete under cyclic compression.

Envelope Curve
The stress-strain curve for monotonic compression was used as the envelope curve for cyclic compression.

Common Point
The reloading path intersects the unloading path at the common point. The strain and stress of the common point (ε_{com}, f_{com}) are related to the strain and stress (ε_{rev}, f_{rev}) where loading reversal occurs as given in Eqs.(22) and (23)

$$\varepsilon_{com} = 0.98\,\varepsilon_{rev} \tag{22}$$

$$f_{com} = 0.9 f_{rev} \tag{23}$$

Unloading Path
Unloading path from the reversal point to the common point is given by a straight line. Unloading path from the common point to the strain axis is given by a parabola with vertex at the zero stress point. The strain of the zero stress point (ε_{res}) is given in Eq.(24)

$$\varepsilon_{res} = 0.65\,\varepsilon_{rev} \tag{24}$$

Reloading Path
Reloading path from the strain axis after a complete unloading to the common point is given by a parabola with the vertex at the zero stress point where the loading resumes. The strain of this point (ε_{rel}) is calculated from Eq.(25)

$$\varepsilon_{rel} = 0.65\,\varepsilon_{res} \tag{25}$$

Reloading path from an unloading path or from the common point to the skeleton curve is given by a straight line from the reloading point through the common point until it reaches the envelope curve.

2.4 Stress-Strain Relationships for Steel

An idealised monotonic curve and a set of hysteretic rules defined by Yokoo and Nakamura (1977) were used as the stress-strain model for steel reinforcement.

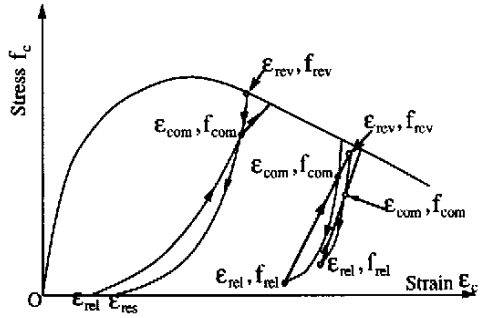

Figure 6: Hysteretic Rules for Cyclic Loading

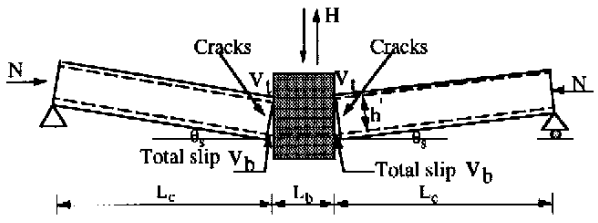

Figure 7: Bar Slip Deformation

3. BAR SLIP DEFORMATION

Under cyclic moment reversal, cracks across the whole column cross sections may form at both stub-faces of the column shown in Fig.1. The reinforcing bars are subjected to cyclic pull-push from both sides of the stub inducing bond deterioration and slippage of steel bars within the stub. Fig.7 shows the fixed end rotation and its resulting lateral deflection due to slippage of steel bars within the stub. The lateral displacement is calculated from Eq.(26).

$$D_s = \frac{v_b - v_t}{h'} L_c \tag{26}$$

in which v_b = total slip of the bottom reinforcement from the stub column interface; v_t = total slip of the top

reinforcement from the stub column interface; h' = distance from top to bottom reinforcing steels; D_s = lateral displacement; L_c= distance from the end support to column stub interface.

An analytical method similar to the model proposed by Filippou et al [1983] was developed to calculate the cummulative slip of steel bar from the stub faces. The mehod is based on finite element approach where the steel bar embedded within the stub is divided into (n-1) elements with equal length. The left end is denoted as 1-st node, whilst the right end as n-th node. There are two unknowns at each node namely the relative slip of steel from the surrounding concrete (v) and the strain in steel (ε_s). Following a mixed two field approximation, the vector of unknowns at the right end is related to the vector of unknowns at the left end as given in Eqs.(27) to (29)

$$z^n = S_n\, z^1 \tag{27}$$

$$S_n = T_n\, T_{n-1} \cdots\cdots T_2 \tag{28}$$

$$T_{i+1} = \begin{bmatrix} -\frac{1}{2}E_{v,i+1}\Psi L & A_s E_{s,i+1} \\ 1 & -\frac{1}{2}L \end{bmatrix}^{-1} \begin{bmatrix} \frac{1}{2}E_{v,1}\Psi L & A_s E_{s,i} \\ 1 & \frac{1}{2}L \end{bmatrix} \tag{29}$$

in which $\mathbf{z}^T = (\Delta v, \Delta\varepsilon_s)$ is the incremental state vector at node; E_v = secant stiffness of bond slip relations; E_s = secant stiffness of stress-strain relations of reinforcing steel; L = the length of element; A_s = the sum of the cross sectional area of all reinforcing bars in one layer; Ψ = the sum of the perimeter of all reinforcing bars in one layer; subscripts i and i+1 indicate the parameter is evaluated at node i and (i+1), respectively.

Bond-slip relations for monotonic loading reported in the literature [Fujii et al, 1994] was used for the envelope curve and the hysteretic rules suggested by Viwathanatepa et al [1979] was used for cyclic loading. By solving Eq.(27) for both top and bottom layers of steel bars, the total slip at both ends (v_b and v_t) are calculated and the bar slip deformation is evaluated from Eq.(26).

4. SHEAR DEFORMATION

Slender beam-columns designed according to the current RC seismic design provisions will have sufficient amount of lateral reinforcement to prevent excessive diagonal tension cracks, hence exhibit small shearing deformation relative to flexural deformation. Therefore, in this research shear deformation was determined using a simplified method suggested by Park and Paulay [1975] that assumes elastic response of RC member to shear.

5. COMPARISON OF THE THEORETICAL PREDICTIONS WITH THE EXPERIMENTAL RESULTS

The accuracy of predictions of the analytical method presented in this paper has been investigated by comparing hysteretic lateral load-lateral displacement curves obtained from the computer program with the experimental results reported in the literatures [Azizinamini et al. 1992 1994, Soesianawati and Park 1988, and Muguruma and Watanabe 1990]. Several selected results are presented in this paper. Figs.8.a. and 8.b. show the lateral load-lateral displacement curves of the specimen D60-15-4-25/8-0,2P [Azizinamini et al.,1994] and specimen Unit-9 [Soesianawati and Park, 1988], respectively. Fig.9. shows the procedure to determine the lateral stress at peak axial load of Unit-9. Fig.10. shows the stress-strain relations of an extreme layer within the core of specimen NC2 [Azizinamini et al. 1992] obtained from the computer output.

5. CONCLUSIONS

An analytical method for the prediction of load-displacement curve of reinforced concrete beam-columns subjected to simulated seismic loading has been presented in this paper. Three deformation components namely flexural, bar-slip and shear deformation were included. The results of the theoretical predictions were verified by comparing the load-displacement curves obtained from the computer program with the experimental results reported in the literatures. This comparative study indicated that the analytical method presented in this paper is capable of predicting the response of reinforced concrete beam-columns to seismic loading with sufficient accuracy.

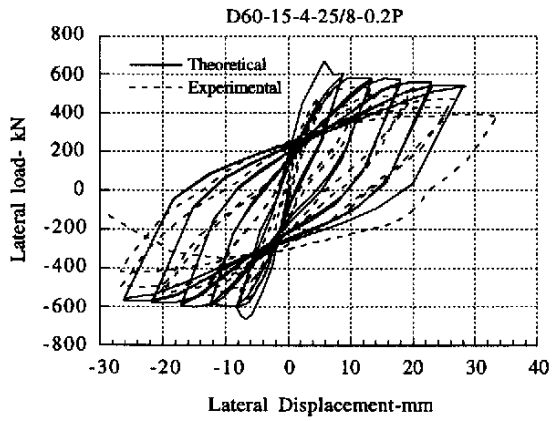

(a): D60-15-4-25/8-0,2P [Azizinamini et al.,1994]

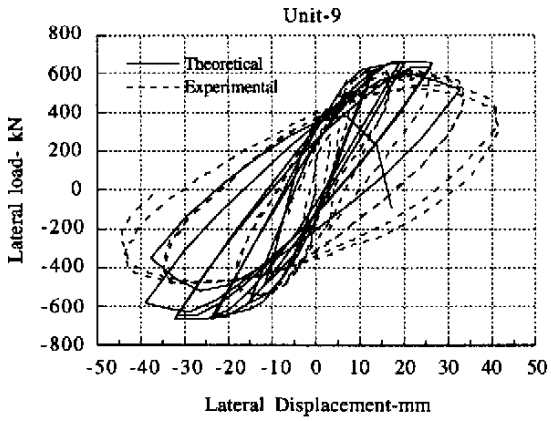

(b): Unit-9 [Soesianawati and Park, 1988]

Figure 8: Load - Displacement Curves

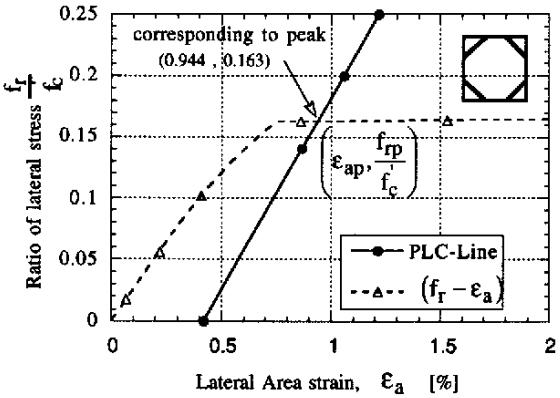

Figure 9: Lateral Stress at Peak of Unit-9

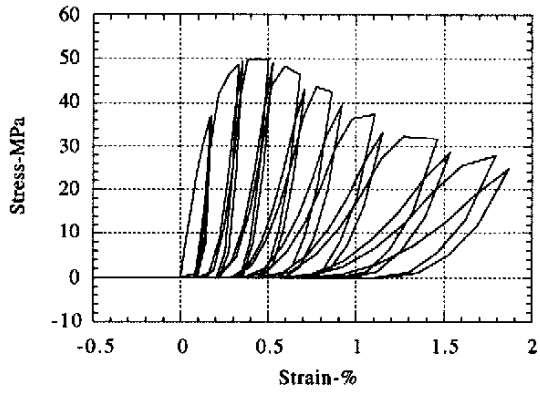

Figure 10: Stress-Strain Relations of Core Concrete Layer

6. REFERENCES

Azizinamini, A., Corley, W.G., and Paul Johal, L.S.(1992), "Effects of Transverse Reinforcement on Seismic Performance of Columns", *ACI Structural Journal*, July-August, pp.442-450

Azizinamini, A., Kuska, S.S.B., Brungardt,P., and Hatfield,E. (1994), "Seismic Behavior of Square High-Strength Concrete Columns", *ACI Structural Journal*, May-June, pp.336-345

Filippou, F.C. , Popov , E.P. , and Bertero, V.V. (1983), "Modeling of R/C Joints Under Cyclic Excitations" . *Journal of Structural Engineering, ASCE*,Vol.109, No.ST11, pp. 2666-2684

Fujii, S., Noguchi, H., and Morita, S.,(1994) "Bond and Anchorage of Reinforcement in High Strength Concrete", *Second US - Japan - New Zealand - Canada Multi-lateral Meeting on Structural Performance of High Strength Concrete in Seismic Regions, Honolulu-Hawaii November 29 - December 1.*

Muguruma, H. , Watanabe, F. , Sakurai, K. , and Nakamura, E. (1979), "Effect of Confinement by High Yield Strength Hoop Reinforcement Upon The Compressive Ductility of Concrete", *Proceedings of The Twenty-Second Japan Congress on Material Research , The Society of Material Science, Japan.*, pp 377-382.

Muguruma,H. , Watanabe,F. , Iwashimizu and Mitsueda,R. (1983) , "Ductility Improvement of High Strength Concrete by Lateral Confinement", Transactions of the Japan Concrete Institute, pp 403-410

Muguruma,H. , and Watanabe, F. (1990), "Ductility Improvement of High-Strength Concrete Columns with Lateral Confinement", *ACI Special Publication SP-121, High Strength Concrete*, pp.47-60

Park , R. and Paulay, T. , (1975), *Reinforced Concrete Structures*, Jhon Wiley and Sons, New York , pp.769.

Soesianawati, M.T., and Park, R. (1988), "Flexural Strength and Ductility of Reinforced Concrete Columns With Various Quantities of Transverse Reinforcement", *Proceedings of Pacific Concrete Conference, New Zealand 8-11 November*, pp.65-76

Viwathanatepa, S,. Popov,E.P., and Bertero, V.V. (1979), *Effects of Generalized Loadings on Bond of Reinforcing Bars Embedded in Confined Concrete Blocks*, Report No.UCB/EERC-79/22 University of California.